

1 **Spatial and temporal variability of urban fluxes of methane, carbon** 2 **monoxide and carbon dioxide above London, UK.**

3

4 Carole Helfter¹, Anja H. Tremper², Christoforos H. Halios³, Simone Kotthaus³, Alex Bjorkegren⁴, C. Sue
5 B. Grimmond³, Janet F. Barlow³, Eiko Nemitz¹

6

7 [1] Centre for Ecology and Hydrology, Penicuik, EH26 0QB, UK

8 [2] MRC-PHE Centre for Environment and Health, King's College London, London, SE1 9NH, UK

9 [3] Department of Meteorology, University of Reading, Earley Gate, PO Box 243, Reading, RG6 6BB, UK

10 [4] King's College London, Strand Campus, London, WC2R 2LS, UK

11

12 *Correspondence to:* Carole Helfter (caro2@ceh.ac.uk)

13

14 **Abstract.** We report on more than three years of measurements of fluxes of methane (CH₄), carbon monoxide (CO) and carbon
15 dioxide (CO₂) taken by eddy-covariance in central London, UK. Mean annual emissions of CO₂ in the period 2012-2014 (39.1
16 ± 2.4 ktons km⁻² y⁻¹) and CO (89 ± 16 tons km⁻² y⁻¹) were consistent (within 1% and 5% respectively) with values from the
17 London Atmospheric Emissions Inventory, but measured CH₄ emissions (72 ± 3 tons km⁻² y⁻¹) were over two-fold larger than
18 the inventory value. Seasonal variability was large for CO with a winter to summer reduction of 69%, and monthly fluxes were
19 strongly anti-correlated with mean air temperature. The winter increment in CO emissions was attributed mainly to vehicle
20 cold starts and reduced fuel combustion efficiency. CO₂ fluxes were 33% higher in winter than in summer and anti-correlated
21 with mean air temperature, albeit to a lesser extent than for CO. This was attributed to an increased demand for natural gas for
22 heating during the winter. CH₄ fluxes exhibited moderate seasonality (21% larger in winter), and a spatially-variable linear
23 anti-correlation with air temperature. Differences in resident population within the flux footprint explained up to 90% of the
24 spatial variability of the annual CO₂ fluxes and up to 99% for CH₄. Furthermore, we suggest that biogenic sources of CH₄,
25 such as wastewater which is unaccounted for by the atmospheric emissions inventories, make a substantial contribution to the
26 overall budget and that commuting dynamics in and out of central business districts could explain some of the spatial and
27 temporal variability of CO₂ and CH₄ emissions. To our knowledge, this study is unique given the length of the datasets
28 presented, especially for CO and CH₄ fluxes. This study offers an independent assessment of “bottom-up” emissions
29 inventories and demonstrates that the urban sources of CO and CO₂ are well characterised in London. This is however not the
30 case for CH₄ emissions which are heavily-underestimated by the inventory approach. Our results and others point to
31 opportunities in the UK and abroad to identify and quantify the “missing” sources of urban methane, revise the methodologies
32 of the emission inventories and devise emission reduction strategies for this potent greenhouse gas.

1 **1 Introduction**

2 The use of eddy-covariance (EC) for the measurement of turbulent fluxes of heat and mass has grown steadily over the past
3 three decades; recently, there were > 400 active sites worldwide (Baldocchi, 2008) spanning six continents. The vast majority
4 of existing sites were established to measure biosphere-atmosphere exchanges of carbon dioxide (CO₂) and heat (Baldocchi et
5 al., 2001). Due to recent technological advances, i.e. the development of new fast response analysers, measurements of eddy-
6 covariance fluxes of other trace gases such as methane (CH₄) and nitrous oxide (N₂O) are gradually being introduced (Crosson,
7 2008; Fiddler et al., 2009; Peltola et al., 2014). With the negotiation of international agreements to greatly reduce greenhouse
8 gas (GHG) emissions by the end of the 21st century, there is an ever increasing need to verify emissions through independent
9 monitoring approaches. Despite 54% of the worldwide population currently living in cities, a figure which could rise to 66%
10 by 2050 (United Nations, 2014), and CO₂ emissions related to urban activities (total of emissions occurring within and outside
11 (e.g. power plants) a conurbation) estimated to represent 70% of the global budget (International Energy Agency, 2012), there
12 have been comparatively few urban studies to evaluate reported GHG emissions. At the time of writing, 61 urban flux towers
13 were listed in the FLUXNET Urban Flux Network database, of which 40 were located in temperate areas (Grimmond and
14 Christen, 2012).

15 At present, most published urban studies have focused on CO₂ at time scales ranging from a few months to a few years (e.g.
16 Christen et al., 2011; Helfter et al., 2011; Pawlak et al., 2011; Jarvi et al., 2012; Liu et al., 2012). Methane, a potent GHG with
17 a global warming potential 28 times larger than that of CO₂ at the 100-year horizon (IPCC, 2013), is receiving increasing
18 attention. Whilst CO₂ emissions are very closely linked to fuel consumption, for which robust statistics can be obtained (at
19 least at country level), CH₄ originates from a much larger range of sources with complex controls. Methane emissions are
20 commonly estimated in “bottom-up” inventories at the national scale (e.g. for IPCC reporting), but also at the urban scale (e.g.
21 London Atmospheric Emissions Inventory in the UK (LAEI, 2013) and the California Air Resources Board (ARB, 2016) in
22 the USA). A variety of techniques have recently been applied to provide independent top-down estimates of urban CH₄
23 emissions. These include ground-based mass balance approaches (McKain et al., 2015), airborne observations (O’Shea et al.,
24 2014; Cambaliza et al., 2015), Fourier Transform Spectrometry (FTS) (Wunch et al., 2009), isotopic source apportionment
25 studies (e.g. Lowry et al., 2001; Zazzeri et al., 2015) and eddy-covariance (Gioli et al., 2012; Pawlak and Fortuniak, 2016).

26 We report on over three years of continuous measurements of fluxes of methane, carbon monoxide and carbon dioxide in the
27 heart of London, UK, the largest European city. This is, to our knowledge, the longest continuous urban record of direct CH₄
28 emission flux measurements. This paper investigates the temporal and spatial emission dynamics of the three pollutants and
29 compares annual budgets with the bottom-up emissions inventory estimates.

30

1 **2 Materials and methods**

2 **2.1 Site description**

3 Fluxes of carbon monoxide (CO), carbon dioxide (CO₂) and methane (CH₄) were measured by eddy-covariance from the
4 rooftop of a 190 m telecommunication tower (BT tower; located at 51° 31' 17.4''N, 0° 8' 20.04''W; Fig. S1) in central London,
5 UK. The measurements, which are ongoing at the time of writing, began in September 2011. The period September 2011 to
6 December 2014 is analysed here. The mean building height in a radius of ca. 10 km from the tower is 8.8 m ± 3.0 m and
7 typically 5.6 m ± 1.8 m for suburban areas (for more details on the local topography and turbulent air flow characteristics of
8 the site see Wood et al., 2010; Evans, 2009). The Greater London area, which extends ca. 20 km in all directions from the BT
9 tower, has a population of 8.6 million (Mayor of London Office, 2015) and population densities in excess of 10⁴ inhabitants
10 km⁻² in the central boroughs.

11 **2.2 Instrumentation**

12 **2.2.1 BT tower site**

13 The eddy-covariance system used at the BT tower consisted of a 3D ultrasonic anemometer (R3-50, Gill Instruments), a Picarro
14 cavity ringdown spectrometer (CRDS) model 1301-f for the measurement of CO₂, CH₄ and H₂O mole fractions and an
15 Aerolaser fast CO monitor model AL5002. The anemometer was mounted on top of a lattice tower located on the roof of the
16 BT tower giving an effective measurement height of 190 m above street level. The two gas analysers were located a few floors
17 below the roof, in an air conditioned room. Air was sampled from ca. 0.3 m below the anemometer head at 20-25 lpm using a
18 45 m long Teflon tube of OD 9.53 mm (3/8''). The Picarro CRDS was fitted with an in-house auto-calibration system and
19 calibrated weekly using two different mixtures of CH₄ and CO₂ in nitrogen (above and below typical ambient concentrations).
20 The anemometer operated at 20 Hz, the CO analyser at 10 Hz and the Picarro CRDS, which was set to sample in 3-species
21 mode, operated at 1 Hz. The data were captured by an in-house LabViewTM (National Instruments) data acquisition program
22 which also controlled the auto-calibration system and fluxes were processed offline by a custom LabView program. Although
23 the Picarro 1301-f has the capability to measure concentrations at 10 Hz, at this rate, this older instrument can only measure
24 two of the three compounds CO₂, CH₄ and H₂O. Because an internal H₂O measurement is required for accurate corrections
25 (e.g. Peltola et al., 2014), this would mean that in fast-response mode the instrument can only measure the flux of CO₂ or CH₄
26 at any one time. Due to the high measurement height, it was found that a response time of 1 Hz was sufficient to capture >70%
27 of the flux (see below).

28 In addition to the closed-path system described above, an open-path infrared gas analyser (IRGA model Li7500, LI-COR
29 Biosciences) measuring CO₂ and H₂O at 20 Hz was mounted next to the ultrasonic anemometer on the roof of the BT tower.
30 Both analysers used the same anemometer but data were processed independently with different eddy-covariance software
31 packages. In the following text, subscripts “_CP” and “_OP” will respectively denote the closed-path and open-path eddy-
32 covariance systems, and fluxes derived from them, located at the BT tower.

1 **2.2.2 King’s College London site**

2 Fluxes of CO₂ measured by EC_{CP} (F_{CO₂CP}) were compared to fluxes measured at an eddy-covariance site at King’s College
3 London (KCL; use of subscript “_KCL” to identify this eddy-covariance system in what follows) Strand campus, 2 km south-
4 east of the BT tower (Fig. S1), where long-term EC measurements have been analysed to study energy exchanges (Kotthaus
5 and Grimmond, 2014a, b), carbon dioxide fluxes (Ward et al., 2015) and the F_{CO₂} storage term in a dense urban environment
6 (Bjorkegren et al., 2015). Carbon dioxide fluxes are obtained from observations of an open-path Li7500 gas analyser and a
7 CSAT3 sonic anemometer (Campbell Scientific). KCL is within the flux footprint of the BT tower during south-easterly wind
8 directions. Fluxes of CO₂ from the KCL site were processed as outlined by Kotthaus and Grimmond (2014a).
9 For the time August – September 2015, a CH₄ sensor (Aerodyne Quantum Cascade Laser (QCL)) was added to the EC system
10 at KCL to also observe F_{CH₄}. No CO was measured at KCL. The EC_{KCL} system was operated at the top of a tower situated on
11 the roof of a large building resulting in a measurement height of 50 m above mean ground level (Ward et al., 2015), i.e. ca.
12 140 m lower than for EC_{CP}. Given that the KCL site is closer to the urban canopy, its source area extends to several hundred
13 metres, while the footprint of the BT tower is much larger, i.e. in the order of kilometres. The QCL measured CH₄, nitrous
14 oxide (N₂O) and water vapour simultaneously and at 10 Hz. The instrument was housed in an air-conditioned cabinet to
15 minimise temperature fluctuations. Air was sampled ca. 20 cm below the anemometer head at 20 lpm through a 25 m long
16 Teflon tube with outer diameter 1.27 cm (1/2”). The data was logged using an in-house LabView program and processed
17 offline as outlined in section 2.3.

18 **2.3 Data processing and filtering**

19 *Half-hourly fluxes*

20 Half-hourly fluxes were calculated using standard eddy-covariance methodology extensively described elsewhere (e.g.
21 Aubinet et al., 2000; Foken et al., 2004; Moncrieff et al., 2004). The quality control procedures and the performance of the
22 eddy-covariance system at the tall tower are presented in sections 2.3.1 to 2.3.3.

23 *Monthly and annual emissions*

24 Monthly emissions were calculated from mean diurnal flux profiles constructed by averaging half-hourly fluxes into 24
25 nominal hourly bins. Annual emissions were estimated by summing monthly averages. However, the data period September
26 2012-March 2013 (no ultrasonic anemometer) was gapfilled using available monthly averages obtained over the remaining
27 measurement period. Due to insufficient temporal coverage, individual annual budgets for 2012-2014 could not be derived for
28 the CO flux. A composite annual emissions estimate was compiled instead which made use of all available monthly averages
29 of F_{CO} over the study period September 2011 to December 2014.

30 **2.3.1 High frequency attenuation**

1 Normalised cospectra ('Co(x)') of wCO₂ and wCH₄ measured by the closed-path system were corrected to match those of wT
2 (where T is sonic temperature) to assess high frequency damping caused by the instrument's limited sampling rate (1 Hz),
3 internal instrument time response and the long inlet line (~ 45 m). Co(wT) followed the theoretical $f^{-5/3}$ (where f denotes
4 frequency) slope for the inertial sub-range (Foken, 2008) over the entire frequency range (Fig. 1). In contrast, Co(wCO₂) and
5 Co(wCH₄) diverged from the theoretical slope for frequencies > 0.1 Hz and followed profiles with slopes of the order of $\sim f^{-5/2}$.
6 Relative humidity did not have a significant influence on Co(wCO₂) and Co(wCH₄) for the two regimes tested (RH = 52%
7 and RH = 80%, data not shown) which suggests that the dominant causes of signal attenuation for our system were the sampling
8 rate and the length of the inlet line. Typical corrections for high frequency attenuation ranged from 15% -30% and based on
9 the co-spectra presented in Fig. 1 it can be inferred that eddies of frequency < 0.1 Hz carried > 70% of the flux measured at
10 the 190 m above-street-level sampling height. The net flux loss resulting from high frequency attenuation was of the order of
11 30% over the entire frequency range. Each half-hourly flux was corrected for high frequency attenuation as part of the offline
12 data processing procedure on a point per point basis.

13

14 **2.3.2 Quality control and filtering**

15 Half-hourly means were excluded if any of the following quality assurance criteria were not fulfilled:

- 16 • The number of raw data points per nominal half hour was < 35000.
- 17 • The flow rate in the sampling line was < 15 lpm (theoretical limit of the transitional phase between laminar and
18 turbulent flow for the sampling tube diameter used in this study).
- 19 • The number of spikes in u, v, w (components of the 3D wind vector measured by the ultrasonic anemometer) or any
20 of the trace gas mole fractions was > 360 (i.e. 1% threshold).
- 21 • Latent and sensible heat fluxes fell outside the -250 W m⁻² to +800 W m⁻² range.
- 22 • The level of turbulence was deemed insufficient for flux measurement (friction velocity, u_* , threshold of 0.2 m s⁻¹).
23 This threshold was used for consistency with previous studies carried out at the BT site (Helfter et al., 2011; Langford
24 et al., 2010).
- 25 • The stationarity test which requires that the difference between the half-hourly flux and the fluxes obtained from 6 x
26 5 min averaging sub-intervals does not exceed 30% is satisfied (Foken and Wichura, 1996; Foken, 2004).

27 **2.3.3 Comparison between closed-path and open-path systems**

28 The performance of the closed-path greenhouse gas eddy-covariance system located on the 35th floor of the BT tower (EC_{CP})
29 was compared to that of the open-path IRGA located on the roof of the tower (EC_{OP}). After frequency correction, half-hourly
30 CO₂ fluxes measured by an open-path Li7500 infrared gas analyser located on the roof of the BT tower (F_{CO₂OP}) were strongly

1 correlated to the fluxes obtained with the closed-path Picarro analyser ($F_{\text{CO}_2_{\text{CP}}}$; Fig. 2). Increased scatter in $F_{\text{CO}_2_{\text{CP}}}$, especially
2 during low fluxes, could be due to uncertainties in determining the time-lag through maximisation of the covariance or also to
3 uncertainties arising from the open-path analyser. The slope of near unity indicates that the high frequency attenuation of the
4 turbulent flow due to instrument response time, sampling flow rate and length of the sampling line was adequately and
5 systematically corrected for.

6 $F_{\text{CO}_2_{\text{CP}}}$ clearly varied with friction velocity (u^*) with maximum fluxes observed at u^* values around 0.8 m s^{-1} , strongly reduced
7 fluxes at low $u^* < 0.3 \text{ m s}^{-1}$ and the indication of reduced values at very high values of u^* (Fig. S2). A similar u^* dependence
8 was found for the fluxes from the open-path gas analyser (not shown). Near-zero fluxes were recorded by both systems for u^*
9 values $< 0.1 \text{ m s}^{-1}$. For CO_2 flux measurements over vegetation, this type of behaviour is usually attributed to a reduction in
10 the transport to the measurement height, resulting in storage of CO_2 below that height which may be subject to advection. In
11 the urban environment, this u^* dependence could alternatively arise from an actual correlation between u^* and surface emission.
12 Indeed, on average both u^* and traffic counts show a minimum at night. However, it is likely that a loss of coupling with street
13 level sources as a result of limited vertical transport occurred in situations of low turbulence. These situations often coincide
14 with stable night-time conditions during which the boundary layer height can approach that of the measurement height (Barlow
15 et al., 2015). In such conditions the measured flux would be an underestimate of the true surface emission due to change in
16 storage in the air column below the measurement height. An explicit treatment of the storage term based on a gradient approach
17 where concentrations and wind speeds are recorded at multiple heights below the EC measurement point could help probe the
18 low u^* regime. Such additional measurements were however not available for the BT tower site and we therefore speculate
19 that the observation of venting after onset of turbulence, when the boundary layer grows, would capture at least some if not
20 most of the material stored below the measurement height.

21

22 **2.4 Uncertainty analysis**

23 Random measurement uncertainties were estimated for each half-hourly averaging period using the Finkelstein and Sims
24 (2001) method and subsequently averaged into monthly means. The upper bounds of the random uncertainties associated with
25 the annual emissions estimates were taken as the maximum monthly random uncertainty for each year and trace gas.

26 Unlike random uncertainties, which arise from instrument noise and representativeness of single-point measurements,
27 systematic errors can be minimised by careful data processing and correction. In particular, successive calibration events were
28 linearly interpolated over time, cancelling out errors due to calibration drifts assuming that the drift was linear over time.

29

30 So far we have considered the error in the local flux. In addition, there is an uncertainty of how this local flux relates to the
31 emission at the surface. The effects of advection and storage on the flux measurement are difficult to quantify in a
32 heterogeneous environment like a city. However, whilst individual half-hourly flux values may be a poor representation of the

1 momentary emission, we expect the errors to reduce significantly when long-term averages are analysed. The validity of this
2 assumption is explored in more detail in what follows.

3 **3 Results and discussion**

4 **3.1 Flux footprint**

5 For consistency with a previous study (Helfter et al., 2011), the flux footprint for the BT tower measurement site was estimated
6 with the analytical model of Kormann and Meixner (2001) for non-neutral atmospheric stratification, under the simplifying
7 assumptions that fluxes of heat and momentum were homogenous across the footprint. The frequency of observation of x_{90} ,
8 the distance from the tower where 90% of the measured fluxes originated from, is shown in Fig. 3 as a function of wind
9 direction and season for the measurement period 2011-2014. The spatial extent of the flux footprint was highly variable over
10 time with recurring seasonal patterns. Typically, 90% of the flux measured at the BT tower site originated from distances of
11 the order of a few km in spring and summer compared to several tens of km in winter. The flux footprint contains two large
12 parks in the SW (Hyde Park, surface area 142 ha) and NW (Regent's Park, surface area 197 ha), sub-urban residential areas in
13 the N, a mixture of heavily urbanised residential and commercial areas in the E and S and a section of the Thames river in the
14 SE.

15 **3.2 Comparison with flux measurements at a lower height**

16 **3.2.1 Temporal similarities**

17 $F_{CO_2_CP}$ and CO_2 fluxes observed at the KCL site ($F_{CO_2_KCL}$) exhibited a high temporal correlation (Fig. 4a, b; averaging period
18 15/09/2011 to 31/12/2013) for diurnal patterns in both winter (defined as December – February) and summer (defined as June
19 – August unless otherwise stated). Daily minima occurred at around 3:00 at both sites which is consistent with minimum traffic
20 loads (Fig. 4f, g). Fluxes tended to increase from ca. 5:00-6:00 until late morning and declined steadily from ca. 18:00 at both
21 sites, which is again in agreement with the declining traffic numbers in the evening. Methane fluxes exhibited similar temporal
22 dynamics with the lowest emissions recorded during the night and a sharp rise between ca. 5:00 and 8:00. A gradual decrease
23 in F_{CH_4} was observed at both sites following the mid-morning maximum.

24 In winter, carbon dioxide fluxes started to increase slightly earlier (by about 30 min on average) at the KCL site. While this
25 time lag was not evident in the summer for F_{CO_2} , methane fluxes started rising later at the elevated measurement point at BT
26 tower even in summer. Boundary layer growth in the morning transition period might explain some of the time delay observed
27 in the carbon fluxes. Mixing height (MH) estimates for several weeks in winter (6 Jan – 11 Feb 2012) and summer (23 July –
28 17 Aug 2012) derived from Doppler LIDAR turbulence measurements (Bohnenstengel et al., 2015) at sites close to BT tower
29 (Fig. 4d, e) indicate that, on average, turbulent mixing extended above the BT tower measurement height of 190 m in both
30 seasons. However, mixing height exhibits great temporal variability depending on the synoptic background conditions; for
31 London it has been found that MH development depends primarily on the boundary layer winds and stability (Halios and

1 Barlow, 2016) so that these short-term climatology estimates might not be representative for the full period analysed for the
2 turbulent fluxes.

3 Growth of the convective layer was rapid in summer and a plateau was typically reached mid-morning which lasted until late
4 afternoon. In agreement with the shorter day-length in winter, growth of the mixing height was slower, collapsing earlier in
5 the evening after the mid-afternoon maximum. Daytime maximum mixing height was about 30% lower in winter compared to
6 the summer. In both summer and winter, traffic counts rose during the morning transition period i.e. before the mixing layer
7 started growing considerably (Fig. 4f, g); in the evening, traffic counts began decreasing after the mixing height had reduced
8 in height. Given that the mean temporal evolution of CO₂ fluxes observed at both KCL and BT tower appeared to be closely
9 linked to the profiles of road traffic, vehicle emissions apparently represent a significant control not only for the local-scale
10 observations at KCL (Ward et al., 2015) but also for fluxes at the elevated BT tower measurement point (Helfter et al., 2011).
11 The slight morning delay in wintertime F_{CO₂} (Fig. 4a) observed at BT tower might be explained by the efficacy of vertical
12 turbulent transport between street level and the top of the BT tower which has been shown to depend on atmospheric stability.
13 The timescale of upward vertical turbulent transport was estimated to be of the order of 10 minutes for near-neutral conditions,
14 increasing to 20-50 minutes for stable conditions (Barlow et al., 2011). Low turbulence and prolonged periods of stable
15 atmospheric stratification (Fig. S3) could thus explain the 1-2 hour lag between the timing of the morning increase in traffic
16 counts and fluxes of CO₂ at the BT tower during the winter (Fig. 4a). This is consistent with the lag time observed for profiles
17 of potential temperature, and thus upward mixing, measured at the BT tower and a lower-level measurement site close to the
18 BT tower at 18 m a.g.l. (Barlow et al., 2015). The near-synchronous rise in CO₂ and CH₄ fluxes observed in summer (summer
19 defined as the months (JJA) in the data period 15/09/2011 - 31/12/2013 for F_{CO₂} and the entire period 19/08 – 01/10/2015 for
20 F_{CH₄}) at the two measurement sites (BT and KCL) at different heights is consistent with an earlier onset of turbulent mixing
21 (Fig. 4 b,c).

22 Storage fluxes are difficult to quantify accurately in a heterogeneous environment like a city as this would require vertical
23 profile measurements below the measurement height at several locations within the flux footprint. The analysis presented here
24 therefore relies to some extent on the assumption that, over long periods, positive and negative storage fluxes cancel out and
25 that effects of advection on the stored quantity are negligible. This assumption is further supported by the very small storage
26 fluxes (< 2.5 % of the magnitude of the vertical fluxes) calculated at the KCL site (Bjorkegren et al., 2015), although these
27 would be somewhat larger for the higher measurement height at BT. While the turbulent fluxes observed at the BT tower and
28 KCL show close temporal alignment (Fig. 4a-c) their absolute values can differ considerably (e.g. KCL-to-BT ratios of peak
29 F_{CO₂} ranged from 1.5 in winter to 0.9 in summer; the summer ratio for F_{CH₄} was 1.5).

30

31 **3.2.2 Comparison of flux spatial variability at the elevated and roof-top sites**

32 Both sites are situated in central London where anthropogenic emissions are high due to the elevated density of people and
33 traffic (Ward et al., 2015). While the source area of the BT site includes central business district (CBD) areas with mostly
34 medium density midrise building structures, residential areas as well as large parks, the KCL footprint is dominated by CBD

1 structures with hardly any vegetation (Kotthaus and Grimmond, 2014b). Only the river Thames in its vicinity reduces
2 anthropogenic emission in some parts of the KCL footprint. To evaluate the response of $F_{CO_2_CP}$ and $F_{CO_2_KCL}$ to variations in
3 source area characteristics, the observations were grouped into eight sectors based on the wind direction measured at the BT
4 tower (Fig. 5). The CO_2 fluxes observed at the two sites are linearly correlated for all eight wind sectors but slopes and goodness
5 of fits vary. This is likely due to differences in flux footprints at the two measurement sites, including the extent (a few km at
6 the BT tower and a few hundred metres at KCL; Kotthaus and Grimmond, 2014b) as well as emission source density (a
7 function of surface types). Near 1:1 agreement was found in the dominant SW wind sector (Fig. 5). For other wind directions,
8 differences in local-scale source area between the two EC sites become apparent: while a large green space (Regent's Park) is
9 located to the NW of BT tower, the surface seen by the KCL measurements is least urbanised towards the S and SE of the site
10 (river Thames; note that busy Waterloo bridge towards the SW of KCL acts as a very strong line source of CO_2 keeping the
11 fluxes relatively high from this wind direction). In response to the surface cover, $F_{CO_2_CP}$ exceeds $F_{CO_2_KCL}$ in the E, S and SE
12 wind sectors by 20%, 50% and 70%, respectively, and is lower by 50%-70% in the N, NW and W sectors with the poorest
13 correlation for the NW sector. The smallest $F_{CO_2_CP}$ fluxes were observed in the NW sector while $F_{CO_2_KCL}$ was highest in
14 sectors NW and W where the particularly busy Aldwych junction is located (Kotthaus and Grimmond, 2014a). KCL falls
15 within the footprint of the BT tower site for SE wind direction, but clearly the BT tower measurement sees additional sources
16 due to the larger footprint. The focus was placed on discussing CO_2 fluxes in this section because it is the only compound for
17 which we have a second long-term flux record at a lower measurement height. Fluxes of CH_4 and CO measured at the BT
18 tower are presented alongside CO_2 in sections 3.3 – 3.5.

19 **3.3 Diurnal variability of the measured fluxes**

20 The fluxes of all three gases (F_{CO} , F_{CO_2} and F_{CH_4}) exhibited well-defined diurnal cycles with minimum emissions during the
21 night, typically from midnight until 5:00 GMT (Fig. 6a-c). Emissions increased sharply from 6:00 reaching a daytime
22 maximum at around 12:00, and then declined steadily until early evening when a local maximum was observed at around
23 18:00-19:00. Mean F_{CH_4} ranged from 5.7 to 11.0 $kg\ km^{-2}\ hour^{-1}$ (maximum-to-minimum ratio of 1.9), F_{CO_2} from 1867 to 6635
24 $kg\ km^{-2}\ hour^{-1}$ (maximum-to-minimum ratio 3.5) and F_{CO} from 4.6 to 16.9 $kg\ km^{-2}\ hour^{-1}$ (maximum-to-minimum ratio 3.7),
25 demonstrating that the relative dynamic range of F_{CH_4} is less than that of the other compounds.

26 The summertime fluxes of CH_4 measured at the 190 m height did lag slightly behind the fluxes observed at the 50 m height,
27 but this apparent delay could have been caused by differences in flux footprint between the sites (e.g. the source area of the
28 BT tower fluxes has a much higher fraction of vegetation cover than the KCL footprint) and the fact that the diurnal profiles
29 were obtained for a much shorter time period (August-September 2015). The similarity in F_{CH_4} temporal dynamics between
30 the two sites supports the idea that the diurnal variations for that gas represent real variability in its source strength rather than
31 an artefact of atmospheric transport as suggested by Gioli et al. (2012) for the Florence (Italy) case study. Indeed, the diurnal
32 variations in F_{CH_4} measured at the BT tower were mirrored by strongly suppressed night-time CH_4 fluxes observed at a much
33 lower height at the KCL site (Fig. 4c), where the storage error has been demonstrated to be small for CO_2 (Bjorkegren et al.,

1 2015). This suggests that fugitive emissions from the natural gas distribution network, which are thought to be the dominant
2 cause of urban CH₄ emissions in developed cities, exhibit diurnal variations and/or that other CH₄ sources with temporal
3 variations (e.g. fugitive emissions from natural gas appliances) are more significant than estimated by LAEI. This is further
4 supported by F_{CH₄} being smaller at the weekend than on weekdays (Fig. 6g).

5

6 **3.3.1 Dependence of flux magnitude and diurnal patterns on wind sector**

7 Segregating emissions by wind direction reveals heterogeneous source distributions at the BT tower site with different temporal
8 patterns (Fig. 6d-f) and source strengths (Fig. S4-S6). The lowest emissions (\pm standard error of the mean) for all three
9 pollutants were recorded for NW winds ($F_{CO} = 1.7 \pm 0.3 \text{ kg km}^{-2} \text{ hour}^{-1}$, $F_{CO_2} = 728 \pm 127 \text{ kg km}^{-2} \text{ hour}^{-1}$, $F_{CH_4} = 1.9 \pm 0.2 \text{ kg}$
10 $\text{km}^{-2} \text{ hour}^{-1}$). The highest emissions of CH₄ were found in the SE wind sector ($17.8 \pm 1.3 \text{ kg km}^{-2} \text{ hour}^{-1}$), in the S sector for
11 CO₂ ($9020 \pm 515 \text{ kg km}^{-2} \text{ hour}^{-1}$) and in the E sector for CO ($25.4 \pm 3.9 \text{ kg km}^{-2} \text{ hour}^{-1}$). The difference in emissions between
12 wind sectors was however only statistically significant for the N and NW wind sectors. Maxima of F_{CO}, F_{CO₂} and F_{CH₄} occurred
13 on average at around 7:00-8:00 in the NW sector. Peak emissions for F_{CO₂} and F_{CH₄} in the remaining wind sectors occurred
14 typically between 9:00 and 12:00. The overall diurnal profile of F_{CO} was bimodal, except for NE and NW, with well-defined
15 mid- to late-morning peaks (typically 9:00 to 12:00 GMT) followed by early evening peaks (17:00 to 19:00). F_{CO} and F_{CO₂}
16 reached night time minima at around 3:00 in all wind sectors whereas F_{CH₄} tended to plateau, except in the SE where emissions
17 tended to increase. The onset of an early morning increase in emissions (ca. 5:00-6:00 GMT) was consistent for all wind
18 directions for F_{CO₂} and F_{CO} but it was less clearly defined for F_{CH₄}. In addition to diurnal trends and dependency on wind sector,
19 emissions of all three pollutants were found to be lower on weekends (Fig. 6g-i), with CH₄ again showing the lowest variability
20 (9% reduction on weekends compared to working days for F_{CH₄}, 22% for F_{CO₂} and 23% for F_{CO}).

21 **3.4 Seasonality of the measured fluxes**

22 For the measurement period September 2011 to December 2014, F_{CH₄}, F_{CO₂} and F_{CO} exhibited marked seasonal cycles with
23 minimum emissions in summer (Fig. 7a-c). The lowest emissions of CO were observed in April but this is thought to be an
24 artefact caused by relatively low temporal and spatial coverage for that month resulting from instrument downtime. Whilst not
25 used in the discussion that follows, the April data point is included in Fig. 7 c and f for consistency. For the months December-
26 February, F_{CO₂} and F_{CH₄} were $4.1 \pm 0.5 \text{ ktons km}^{-2} \text{ month}^{-1}$ and $7.4 \pm 0.8 \text{ tons km}^{-2} \text{ month}^{-1}$, respectively, and decreased to 2.7
27 $\pm 0.3 \text{ ktons km}^{-2} \text{ month}^{-1}$ (33% reduction) and $5.8 \pm 0.4 \text{ tons km}^{-2} \text{ month}^{-1}$ (21% reduction), respectively, in summer (June-
28 August). The difference between winter and summertime emissions of CO was 3-fold with $9.1 \pm 2.5 \text{ tons km}^{-2} \text{ month}^{-1}$ in
29 December-February and $2.9 \pm 0.1 \text{ tons km}^{-2} \text{ month}^{-1}$ in June-July (due to instrument downtime, no data are available for
30 August).

31

32 **3.4.1 Seasonal controls of fluxes of carbon monoxide and carbon dioxide**

1 It is well established that emissions of CO from petrol cars are temperature dependent, e.g. increasing by a factor of 5-6 at
2 ambient temperature 0 °C compared to 25 °C (Andrews, 2004) during the first 5-10 minutes following engine warm-up. The
3 strong negative linear dependence of F_{CO} upon air temperature (Fig. 7f) could thus indicate that cold starts and reduced
4 combustion efficiency played an important role during winter. Winter time (December-February) emissions of CO accounted
5 for 45% of the annual budget for this pollutant which is consistent with LAEI (LAEI, 2013) estimates of the combined natural
6 gas and cold start contribution to annual CO emissions (total 32%, with 26% and 6% attributed to cold starts and natural gas
7 consumption, respectively). F_{CO_2} was also correlated with air temperature (Fig. 7e; $R^2 = 0.59$), albeit to a lesser extent than
8 F_{CO} , which reflected the seasonal changes in domestic and commercial natural gas usage, but may also be influenced by
9 increased photosynthetic uptake by vegetation in the footprint during the warmer months. Anti-correlations between monthly
10 F_{CO_2} and air temperature have been reported in other studies (e.g. Beijing, Liu et al., 2012; London, Ward et al., 2015). The
11 gradient between F_{CO_2} and air temperature observed in this study ($-0.94 \mu\text{mol m}^{-2} \text{s}^{-1} \text{ } ^\circ\text{C}^{-1}$) falls between the values reported
12 for the London site ($-1.95 \mu\text{mol m}^{-2} \text{s}^{-1} \text{ } ^\circ\text{C}^{-1}$) and the Beijing site ($-0.34 \mu\text{mol m}^{-2} \text{s}^{-1} \text{ } ^\circ\text{C}^{-1}$).

13 The flux ratio of CO to CO_2 is of the order of 4 mmol mol^{-1} in winter (excess CO due to cold starts and incomplete combustion)
14 and 2 mmol mol^{-1} in summer despite only moderate seasonal variations in traffic loads (Fig. S7). Traffic loads at Marylebone
15 Road, one of the busiest arteries in central London located $< 1 \text{ km}$ north of the BT Tower, varied by less than 5% seasonally
16 in the period June 2012 to December 2014 (source Transport for London; personal communication). The seasonality of F_{CO_2}
17 is hence likely controlled by changes in natural gas consumption and vegetation (Gioli et al., 2012; Helfter et al., 2011). This
18 is further supported by relatively constant ratios of F_{CH_4} to F_{CO_2} which suggests that seasonal variations in emissions were of
19 comparable magnitude for these two gases (Fig. S7). On average over the full three years of the study (2012-2014),
20 summertime F_{CO_2} were 30% lower than in winter (29% in 2012, 30% in 2013 and 2014). In comparison, during an earlier study
21 at the same site covering the year 2007, the winter to summer decrement was only 20% (Helfter et al., 2011).

22

23 **3.4.2 Seasonal controls of methane emissions**

24 Fluxes of CH_4 were 17% lower in summer than in winter (18%, 12% and 20% for 2012, 2013 and 2014 respectively) and the
25 linear correlation of monthly averages with temperature was not statistically significant (Fig. 7d; $R^2 = 0.31$, p-value = 0.06).
26 In contrast, the winter to summer decrease was of the order of 63% in the city of Łódź, Poland (Pawlak and Fortuniak, 2016)
27 and the dependence of F_{CH_4} upon air temperature was statistically significant. The weaker correlation of F_{CH_4} with air
28 temperature in London suggests that the total methane flux is due to a superposition of sources with constant and time-varying
29 emission rates, whereas in Florence (Italy) no significant seasonality in CH_4 emissions was observed (Gioli et al., 2012). They
30 related this to a constant pressure in the gas distribution network serving Florence. However, seasonality in both CH_4
31 concentrations and isotopic signature have been reported in the Greater London area (Lowry et al., 2001). The winter time
32 increase above background in CH_4 concentrations and the accompanying enrichment in $\delta^{13}C$ were consistent with North Sea
33 natural gas and attributed to losses of CH_4 from over-pressurised pipelines in response to (or anticipation of) an increase in

1 demand and to incomplete combustion upon boiler ignition. The seasonality of F_{CH_4} in Łódź (Poland) was also attributed to
2 variations in natural gas usage (Pawlak and Fortuniak, 2016). Urban CH_4 emissions in Boston (USA) attributed to natural gas
3 use also displayed a modest, albeit not statistically significant, seasonality, with lower emissions during the summer (McKain
4 et al., 2015). An increase of total CH_4 emissions in summer could indicate temperature-sensitive biogenic sources played an
5 important role in Boston. Although individually small, fugitive post-meter emissions (i.e. in homes or work place) can make
6 a non-negligible cumulative contribution at the city scale (Wennberg et al., 2012). Post-meter emissions are made up of time-
7 varying (incomplete combustion upon natural gas appliance ignition/ usage) and constant components (leaking valves/ fittings)
8 which contribute to both the seasonal variability and to the baseline of CH_4 emissions. Finally, methane emissions from
9 liquefied petroleum gas (LPG) vehicles, although small compared to natural gas emissions, exhibit a positive dependence upon
10 temperature (Nam et al., 2004) and are expected to also contribute to the seasonality and diurnal variation of the total urban
11 CH_4 fluxes.

12 **3.5 Annual budgets of methane, carbon monoxide and carbon dioxide emissions**

13 Annual emissions of CO_2 ranged from 36.3 to 40.7 ktons $\text{km}^{-2} \text{y}^{-1}$ with a 3-year mean of 39.1 ± 2.4 ktons $\text{km}^{-2} \text{y}^{-1}$ (Table 1).
14 These values are in good agreement with results from a previous measurement campaign at the BT tower in 2007 (35.5 ktons
15 $\text{km}^{-2} \text{y}^{-1}$; Helfter et al., 2011) and London Atmospheric Emissions Inventory (LAEI) bottom-up emission estimates for the
16 central London boroughs of Westminster and Camden, which are the foremost spatial source areas entrained by the BT tower
17 flux footprint. The good agreement for CO_2 obtained in the present and previous studies using different instrumentation
18 provides a benchmark for subsequent comparisons between top-down measurements and bottom-up inventory estimates. Due
19 to insufficient temporal coverage, individual annual budgets for 2012-2014 could not be derived for CO. Instead, one single
20 annual CO flux value was calculated from individual monthly averages collected in the period September 2011 – December
21 2014 on the assumption that year-on-year variability was small. Furthermore, emissions of CO for August and September,
22 when no observations were available, were estimated from a linear relation between F_{CO} and air temperature (Fig. 7f). The
23 composite annual emissions estimate of $89 \pm 16 \text{ t km}^{-2} \text{y}^{-1}$ (range taken as the random uncertainty) is consistent with the LAEI
24 data (Table 1).

25 Flux ratios are less sensitive to limitations in vertical transport and provide an additional means of assessing the quality of the
26 bottom-up emission inventories and identifying poorly represented sources. Measured flux ratios of F_{CO} to F_{CO_2} were consistent
27 with average LAEI emission ratios (Table 2, Fig. S9). Measured flux ratios of F_{CO} to F_{CH_4} were about half the inventoried
28 values and measured ratios of F_{CH_4} to F_{CO_2} were twice the mean LAEI values (Table 2; Fig. S8), consistent with the measured
29 annual CH_4 fluxes (3-year mean $72 \pm 3 \text{ t km}^{-2} \text{y}^{-1}$) being more than twice the inventory value. This indicates that some CH_4
30 sources were either underestimated or unaccounted for by the LAEI. Of the source categories included in the LAEI and listed
31 in Table 2 only gas leakage has the potential to increase the CH_4/CO_2 flux ratio, but an underestimation in leakage is only a
32 possible explanation if it follows the measured diurnal cycle, either due to changes in the supply pressure or in post-meter
33 emissions. We speculate that the diurnal, seasonal and spatial variations in F_{CH_4} , and the larger $F_{\text{CH}_4}/F_{\text{CO}_2}$ ratio could be due a

1 contribution of temperature-sensitive CH₄ emissions perhaps of biogenic origin (e.g. increased methanogenesis from sewerage)
2 not included in the inventories. This could explain why the net seasonal decrease in CH₄ was but half that of CO₂ (Fig. 7a and
3 b). Previously reported discrepancies of 1.5 to > 2 between top-down and bottom-up estimates of CH₄ for the South Coast Air
4 Basin in the greater Los Angeles (USA) area have been related to emissions from landfills and other biogenic sources (Hsu et
5 al., 2010; Wunch et al., 2009). In our study, annual methane fluxes exhibited substantial spatial variability when segregated
6 by wind sector (Fig. 8a). Fluxes of methane in the E, S and SE sectors were ca. 30% larger than the mean annual F_{CH₄} estimate
7 and exceeded the top boundary of the overall mean (taken as mean F_{CH₄} + maximum monthly uncertainty; Fig. 8a). In contrast,
8 F_{CH₄} from the N and NW sectors were 40% and 30% of the mean value, respectively, and fell below the lower limit of the
9 overall mean (taken as mean F_{CH₄} – maximum monthly uncertainty). This perhaps suggests more complex, spatially discrete,
10 source distribution and composition for CH₄ compared with CO₂ and CO. The linear correlation between F_{CH₄} and population
11 was strong if the highest emitting wind sectors (E, S and SE) were excluded from the regression (Fig. 8b). Socio-economic
12 temporal dynamics, such as a significant daytime influx of commuters into a business district (e.g. the City of London financial
13 district which is located 3-4 km S-SE of the BT tower), might contribute substantially to CH₄ emissions (e.g. from sewage,
14 natural gas); in addition, the measured CH₄ emissions from such business areas might bear no correlation with the actual
15 resident population reported here (source: London Datastore, Greater London Authority, 2016) which can be considerably
16 smaller than the commuting workforce. Emissions of CH₄ in the E were strongly correlated with air temperature (Table 3),
17 which suggests one or more dominant seasonal source in that wind sector. Finally, neither test was statistically significant for
18 emissions in the SE and S where the flux footprints entrain some of the most heavily urbanised areas of central London as well
19 as part of the river Thames. Further work is needed to investigate the potential presence of additional sources of CH₄ which
20 might be prevalent in those wind sectors.

21 As for CH₄, CO₂ fluxes exhibited a dependence upon air temperature in the N, NE, E and W. The seasonality of the CO₂
22 emissions was not statistically significant in the remaining wind sectors which might be due to the presence of substantial
23 constant sources of CO₂ or to the prevalence of seasonal activities which do not emit CO₂ locally (e.g. more electrical heating
24 than natural gas). However, the spatial variability of F_{CO₂} was well-captured by differences in population in the respective flux
25 footprints of all wind sectors, except S (Fig. 8b).

26 **4 Conclusions**

27 This study presents the results of more than three years of continuous long-term eddy-covariance observations of fluxes of
28 CO, CO₂ and CH₄ at an elevated measurement site (BT tower, 190 m a.g.l.) in central London, UK. This unique vantage point,
29 combined with the length of the study, allowed for the spatial and temporal emission dynamics to be analysed in detail. The
30 main conclusions are that all three trace gases exhibited diurnal cycles consistent with anthropogenic activities (traffic, natural
31 gas use) and underwent marked seasonal dynamics, with reduced emissions in the summer.

1 Emissions of CO were strongly correlated with air temperature which is thought to be due to cold starts and reduced fuel
2 combustion efficiency by the London fleet during the winter. Winter time emissions of CO accounted for 45% of the annual
3 budget. Emissions of CO₂ were also correlated to air temperature and were 33% larger in winter than in summer. CO₂ emissions
4 were predominantly controlled by the seasonal increase in natural gas consumption, although vegetation uptake would also
5 have lowered CO₂ fluxes in summer. CH₄ fluxes averaged over all wind sectors decreased by 21% between winter and summer
6 but unlike CO and CO₂, the correlation with air temperature was not statistically significant. . When segregated by wind sector,
7 CH₄ fluxes in the E and W were strongly correlated with air temperature suggestive of sources with highly seasonal emission
8 rates, possibly leaks from the natural gas distribution network or emissions from sewage. Furthermore, CO₂ and CH₄ fluxes
9 were positively correlated with population density in all wind sectors except S for F_{CO2} and S, SE and E for F_{CH4}. This indicates
10 heterogeneous source distributions and/or densities with temporal dynamics which differ from the other wind sectors.
11 Measured annual emissions of CO₂ (39 ktons km⁻²) were in good agreement with bottom-up estimates from the London
12 Atmospheric Emissions Inventory (LAEI). As CO₂ is the most accurately represented of the three compounds in emission
13 inventories, this provides confidence in the flux measurements. Similarly, the measured annual budget for CO (89 tons km⁻²)
14 was consistent with LAEI values which confirms that the spatial distribution of the sources of this pollutant is well captured
15 by the inventory. However, the measured annual CH₄ emissions (72 tons km⁻²) were more than double the LAEI value
16 suggesting that sources are not as well-characterised by the inventory. In particular, we hypothesise that the shortfall in
17 inventoried CH₄ emissions can be explained by the existence of temperature-dependent sources related to natural gas usage
18 and perhaps also of biogenic origin (e.g. sewage).

19 **Acknowledgements**

20 The authors acknowledge a succession of projects for funding this research (NERC-funded projects ClearfLo (H003231/1),
21 GAUGE (NE/K002279/1)) as well as support by NERC National Capability funding, the EU FP7 Infrastructure Project InGOS
22 project (284274), the EU FP7 Grant BRIDGE (211345), and King's College London.

23 The authors also acknowledge British Telecom (BT) for granting use of the tall tower for research purposes. In particular, we
24 are grateful to Karen Ahern for arranging work permits and facilitating access to the site. Thank you also to aerial riggers
25 Robert Semon, Wayne Loeber and Mark West for help with the installation and maintenance of the rooftop instruments. We
26 are grateful to BT security and facilities staff for their continued support and assistance with day-to-day logistics and to Dr
27 Neil Mullinger (Centre for Ecology and Hydrology) for help with instrument maintenance and visits to the site. Supporting the
28 KCL observations, we thank Dr Arnold Moene at Wageningen University for providing the ECpack software; all staff and
29 students at KCL and University of Reading (Grimmond group) who contributed to the data collection; KCL Directorate of
30 Estates and Facilities for giving us the opportunity to operate the various measurement sites.

31

1 **References**

2 ARB (Air Resources Board), California Environment Protection Agency, <http://www.arb.ca.gov/ei/ei.htm>, 2016.

3

4 Andrews, G. E., Zhu, G., Li, H., Simpson, A., Wylie, J.A., Bell, M. and Tate, J. : The effect of ambient temperature on cold
5 start urban traffic emissions for a real world SI car, Proceedings of SAE 2004 Powertrain & Fluid Systems Conference and
6 Exhibition Tampa, FL, USA, October 2004, 2004.

7

8 Aubinet, M., Grelle, A., Ibrom, A., Rannik, U., Moncrieff, J., Foken, T., Kowalski, A. S., Martin, P. H., Berbigier, P.,
9 Bernhofer, C., Clement, R., Elbers, J., Granier, A., Grunwald, T., Morgenstern, K., Pilegaard, K., Rebmann, C., Snijders, W.,
10 Valentini, R., and Vesala, T.: Estimates of the annual net carbon and water exchange of forests: The EUROFLUX
11 methodology, *Advances in Ecological Research*, Vol 30, 30, 113-175, 2000.

12

13 Baldocchi, D., Falge, E., Gu, L. H., Olson, R., Hollinger, D., Running, S., Anthoni, P., Bernhofer, C., Davis, K., Evans, R.,
14 Fuentes, J., Goldstein, A., Katul, G., Law, B., Lee, X. H., Malhi, Y., Meyers, T., Munger, W., Oechel, W., U, K. T. P.,
15 Pilegaard, K., Schmid, H. P., Valentini, R., Verma, S., Vesala, T., Wilson, K., and Wofsy, S.: Fluxnet: A new tool to study the
16 temporal and spatial variability of ecosystem-scale carbon dioxide, water vapor, and energy flux densities, *Bulletin of the*
17 *American Meteorological Society*, 82, 2415-2434, 10.1175/1520-0477(2001)082<2415:fanfts>2.3.co;2, 2001.

18

19 Baldocchi, D.: Breathing of the terrestrial biosphere: Lessons learned from a global network of carbon dioxide flux
20 measurement systems, *Australian Journal of Botany*, 56, 1-26, 10.1071/bt07151, 2008.

21

22 Barlow, J. F., Dunbar, T. M., Nemitz, E. G., Wood, C. R., Gallagher, M. W., Davies, F., O'Connor, E., and Harrison, R. M.:
23 Boundary layer dynamics over London, UK, as observed using Doppler LIDAR during REPARTEE-II, *Atmospheric*
24 *Chemistry and Physics*, 11, 2111-2125, 10.5194/acp-11-2111-2011, 2011.

25

26 Barlow, J. F., Halios, C. H., Lane, S. E., and Wood, C. R.: Observations of urban boundary layer structure during a strong
27 urban heat island event, *Environmental Fluid Mechanics*, 15, 373-398, 10.1007/s10652-014-9335-6, 2015.

28

29 Bjorkegren, A. B., Grimmond, C. S. B., Kotthaus, S., and Malamud, B. D.: CO₂ emission estimation in the urban environment:
30 Measurement of the CO₂ storage term, *Atmospheric Environment*, 122, 775-790,
31 <http://dx.doi.org/10.1016/j.atmosenv.2015.10.012>, 2015.

32

1 Bohnenstengel, S. I., Belcher, S. E., Aiken, A., Allan, J. D., Allen, G., Bacak, A., Bannan, T. J., Barlow, J. F., Beddows, D.
2 C. S., Bloss, W. J., Booth, A. M., Chemel, C., Coceal, O., Di Marco, C. F., Dubey, M. K., Faloon, K. H., Fleming, Z. L.,
3 Furger, M., Gietl, J. K., Graves, R. R., Green, D. C., Grimmond, C. S. B., Halios, C. H., Hamilton, J. F., Harrison, R. M., Heal,
4 M. R., Heard, D. E., Helfter, C., Herndon, S. C., Holmes, R. E., Hopkins, J. R., Jones, A. M., Kelly, F. J., Kotthaus, S.,
5 Langford, B., Lee, J. D., Leigh, R. J., Lewis, A. C., Lidster, R. T., Lopez-Hilfiker, F. D., McQuaid, J. B., Mohr, C., Monks, P.
6 S., Nemitz, E., Ng, N. L., Percival, C. J., Prevot, A. S. H., Ricketts, H. M. A., Sokhi, R., Stone, D., Thornton, J. A., Tremper,
7 A. H., Valach, A. C., Visser, S., Whalley, L. K., Williams, L. R., Xu, L., Young, D. E., and Zotter, P.: Meteorology, air quality,
8 and health in London the ClearfLo project, *Bulletin of the American Meteorological Society*, 96, 779-804, 10.1175/bams-d-
9 12-00245.1, 2015.

10

11 Cambaliza M.O.L., S. P., Bogner J., Caulton D.R., Stirn B., et al.: Quantification and source apportionment of the methane
12 emission flux from the city of Indianapolis., *Elementa Science of the Anthropocene*, 3, 10.12952/journal.elementa.000037,
13 2015.

14

15 Carslaw, D. C. and Ropkins K.: openair --- an R package for air quality data analysis. *Environmental Modelling & Software*.
16 Volume 27-28, 52-61, 2012.

17

18 Carslaw D.C. and Ropkins K.: openair: Open-source tools for the analysis of air pollution data. R package version 1.7-
19 3, <http://CRAN.R-project.org/package=openair>, 2016.

20

21 Christen, A., Coops, N. C., Crawford, B. R., Kellett, R., Liss, K. N., Olchovski, I., Tooke, T. R., van der Laan, M., and Voegt,
22 J. A.: Validation of modeled carbon-dioxide emissions from an urban neighborhood with direct eddy-covariance
23 measurements, *Atmospheric Environment*, 45, 6057-6069, 10.1016/j.atmosenv.2011.07.040, 2011.

24

25 Christen, A.: Atmospheric measurement techniques to quantify greenhouse gas emissions from cities, *Urban Climate*, 10, Part
26 2, 241-260, <http://dx.doi.org/10.1016/j.uclim.2014.04.006>, 2014.

27

28 Crosson, E. R.: A cavity ring-down analyzer for measuring atmospheric levels of methane, carbon dioxide, and water vapor,
29 *Applied Physics B-Lasers and Optics*, 92, 403-408, 10.1007/s00340-008-3135-y, 2008.

30

31 Evans, S.: 3D cities and numerical weather prediction models: An overview of the methods used in the LUCID project,
32 available at <http://discovery.Ucl.Ac.Uk/17404/1/17404.Pdf> UCL Working Paper Series, 2009.

33

1 Fiddler, M. N., Begashaw, I., Mickens, M. A., Collingwood, M. S., Assefa, Z., and Bililign, S.: Laser spectroscopy for
2 atmospheric and environmental sensing, *Sensors*, 9, 10447-10512, 10.3390/s91210447, 2009.

3

4 Finkelstein, P. L., and Sims, P. F.: Sampling error in eddy correlation flux measurements, *Journal of Geophysical Research:*
5 *Atmospheres*, 106, 3503-3509, 10.1029/2000jd900731, 2001.

6

7 Foken, T., and Wichura, B.: Tools for quality assessment of surface-based flux measurements, *Agricultural and Forest*
8 *Meteorology*, 78, 83-105, 10.1016/0168-1923(95)02248-1, 1996.

9

10 Foken, T.: *Micrometeorology*, Springer-Verlag Berlin Heidelberg, 308 pp., 2008.

11 Foken, T., Gödecke, M., Mauder, M., Mahrt, L., Amiro, B., and Munger, W.: Post-field data quality control, in: *Handbook of*
12 *micrometeorology*, edited by: Lee, X., Kluwer Academic Publishers, 2004.

13

14 Gioli, B., Toscano, P., Lugato, E., Matese, A., Miglietta, F., Zaldei, A., and Vaccari, F. P.: Methane and carbon dioxide fluxes
15 and source partitioning in urban areas: The case study of Florence, Italy, *Environmental Pollution*, 164, 125-131,
16 10.1016/j.envpol.2012.01.019, 2012.

17

18 Greater London Authority, London Datastore: <http://data.london.gov.uk/>, 2016.

19

20 Grimmond, C. S. B., and Christen, A.: Flux measurements in urban ecosystems, in: *FluxLetter*, The newsletter of FLUXNET,
21 1, FLUXNET, 2012.

22

23 Halios, C. H., and Barlow, J. F.: Observations of the morning development of the urban boundary layer over London, UK,
24 taken during the ACTUAL project. , *Boundary-Layer Meteorology*, under review 2016.

25

26 Harrison, R. M., Dall'Osto, M., Beddows, D. C. S., Thorpe, A. J., Bloss, W. J., Allan, J. D., Coe, H., Dorsey, J. R., Gallagher,
27 M., Martin, C., Whitehead, J., Williams, P. I., Jones, R. L., Langridge, J. M., Benton, A. K., Ball, S. M., Langford, B., Hewitt,
28 C. N., Davison, B., Martin, D., Petersson, K. F., Henshaw, S. J., White, I. R., Shallcross, D. E., Barlow, J. F., Dunbar, T.,
29 Davies, F., Nemitz, E., Phillips, G. J., Helfter, C., Di Marco, C. F., and Smith, S.: Atmospheric chemistry and physics in the
30 atmosphere of a developed megacity (London): an overview of the REPARTEE experiment and its conclusions, *Atmospheric*
31 *Chemistry and Physics*, 12, 3065-3114, 2012.

32

1 Helfter, C., Famulari, D., Phillips, G. J., Barlow, J. F., Wood, C. R., Grimmond, C. S. B., and Nemitz, E.: Controls of carbon
2 dioxide concentrations and fluxes above central London, *Atmospheric Chemistry and Physics*, 11, 1913-1928, 10.5194/acp-
3 11-1913-2011, 2011.

4

5 Hsu, Y.-K., VanCuren, T., Park, S., Jakober, C., Herner, J., FitzGibbon, M., Blake, D. R., and Parrish, D. D.: Methane
6 emissions inventory verification in Southern California, *Atmospheric Environment*, 44, 1-7, 10.1016/j.atmosenv.2009.10.002,
7 2010.

8

9 International Energy Agency: World energy outlook, [http://www.iea.org/publications/freepublications/publication/world-](http://www.iea.org/publications/freepublications/publication/world-energy-outlook-2012.html)
10 [energy-outlook-2012.html](http://www.iea.org/publications/freepublications/publication/world-energy-outlook-2012.html), 2012.

11

12 IPCC (International Panel on Climate Change): IPCC fifth assessment report: Climate change 2013, 2013.

13

14 Jarvi, L., Nordbo, A., Junninen, H., Riikonen, A., Moilanen, J., Nikinmaa, E., and Vesala, T.: Seasonal and annual variation
15 of carbon dioxide surface fluxes in Helsinki, Finland, in 2006-2010, *Atmospheric Chemistry and Physics*, 12, 8475-8489,
16 10.5194/acp-12-8475-2012, 2012.

17

18 Kormann, R., and Meixner, F. X.: An analytical footprint model for non-neutral stratification, *Boundary-Layer Meteorology*,
19 99, 207-224, 10.1023/a:1018991015119, 2001.

20

21 Kotthaus, S., and Grimmond, C. S. B.: Identification of micro-scale anthropogenic CO₂, heat and moisture sources - processing
22 eddy covariance fluxes for a dense urban environment, *Atmospheric Environment*, 57, 301-316,
23 10.1016/j.atmosenv.2012.04.024, 2012.

24

25 Kotthaus, S., and Grimmond, C. S. B.: Energy exchange in a dense urban environment – part II: Impact of spatial heterogeneity
26 of the surface, *Urban Climate*, 10, Part 2, 281-307, <http://dx.doi.org/10.1016/j.uclim.2013.10.001>, 2014a.

27

28 Kotthaus, S., and Grimmond, C. S. B.: Energy exchange in a dense urban environment – part I: Temporal variability of long-
29 term observations in central London, *Urban Climate*, 10, Part 2, 261-280, <http://dx.doi.org/10.1016/j.uclim.2013.10.002>,
30 2014b.

31

32 Langford, B., Nemitz, E., House, E., Phillips, G. J., Famulari, D., Davison, B., Hopkins, J. R., Lewis, A. C., and Hewitt, C.
33 N.: Fluxes and concentrations of volatile organic compounds above central London, UK, *Atmospheric Chemistry and Physics*,
34 10, 627-645, 10.5194/acp-10-627-2010, 2010.

1 LAEI (London Atmospheric Emissions Inventory), London Datastore, [http://data.london.gov.uk/dataset/london-atmospheric-](http://data.london.gov.uk/dataset/london-atmospheric-emissions-inventory-2013)
2 [emissions-inventory-2013](http://data.london.gov.uk/dataset/london-atmospheric-emissions-inventory-2013), 2013.
3
4 Liu, H. Z., Feng, J. W., Jarvi, L., and Vesala, T.: Four-year (2006-2009) eddy covariance measurements of CO₂ flux over an
5 urban area in Beijing, *Atmospheric Chemistry and Physics*, 12, 7881-7892, 10.5194/acp-12-7881-2012, 2012.
6
7 Lowry, D., Holmes, C. W., Rata, N. D., O'Brien, P., and Nisbet, E. G.: London methane emissions: Use of diurnal changes in
8 concentration and delta C-13 to identify urban sources and verify inventories, *Journal of Geophysical Research-Atmospheres*,
9 106, 7427-7448, 10.1029/2000jd900601, 2001.
10
11 McKain, K. K., Down, A., Raciti, S. M., Budney, J., Hutyra, L. R., Floerchinger, C., Herndon, S. C., Nehr Korn, T., Zahniser,
12 M. S., Jackson, R. B., Phillips, N., and Wofsy, S. C.: Methane emissions from natural gas infrastructure and use in the urban
13 region of Boston, Massachusetts, *Proceedings of the National Academy of Sciences of the United States of America*, 112,
14 1941-1946, 10.1073/pnas.1416261112, 2015.
15
16 Nam, E. K., Jensen, T. E., and Wallington, T. J.: Methane emissions from vehicles, *Environmental Science & Technology*, 38,
17 2005-2010, 10.1021/es034837g, 2004.
18
19 Moncrieff, J., Clement, R., Finnigan, J., and Meyers, T.: Averaging, detrending and filtering of eddy covariance time series.
20 In: *Handbook of Micrometeorology*, Lee, X. (Ed.), Kluwer Academic Publishers, 2004.
21
22 O'Shea, S. J., Allen, G., Fleming, Z. L., Bauguitte, S. J. B., Percival, C. J., Gallagher, M. W., Lee, J., Helfter, C., and Nemitz,
23 E.: Area fluxes of carbon dioxide, methane, and carbon monoxide derived from airborne measurements around greater London:
24 A case study during summer 2012, *Journal of Geophysical Research-Atmospheres*, 119, 4940-4952, 10.1002/2013jd021269,
25 2014.
26
27 Mayor of London Office: London population confirmed at record high: [https://www.london.gov.uk/media/mayor-press-](https://www.london.gov.uk/media/mayor-press-releases/2015/02/london-population-confirmed-at-record-high)
28 [releases/2015/02/london-population-confirmed-at-record-high](https://www.london.gov.uk/media/mayor-press-releases/2015/02/london-population-confirmed-at-record-high), 2015.
29
30 Pawlak, W., Fortuniak, K., and Siedlecki, M.: Carbon dioxide flux in the centre of Lodz, Poland - analysis of a 2-year eddy
31 covariance measurement data set, *International Journal of Climatology*, 31, 232-243, 10.1002/joc.2247, 2011.
32
33 Pawlak, W. and Fortuniak, K.: Eddy covariance measurements of the net turbulent methane flux in the city centre – results of
34 2 years campaign in Łódź, Poland, *Atmos. Chem. Phys. Discuss.*, 2016, 1-38, 2016.

1

2 Peltola, O., Hensen, A., Helfter, C., Marchesini, L. B., Bosveld, F. C., van den Bulk, W. C. M., Elbers, J. A., Haapanala, S.,
3 Holst, J., Laurila, T., Lindroth, A., Nemitz, E., Rockmann, T., Vermeulen, A. T., and Mammarella, I.: Evaluating the
4 performance of commonly used gas analysers for methane eddy covariance flux measurements: The InGOS inter-comparison
5 field experiment, *Biogeosciences*, 11, 3163-3186, 10.5194/bg-11-3163-2014, 2014.

6

7 United Nations: World urbanization prospects, <http://esa.un.org/unpd/wup/highlights/wup2014-highlights.pdf>, 2014.

8

9 Ward, H. C., Kotthaus, S., Grimmond, C. S. B., Bjarkegren, A., Wilkinson, M., Morrison, W. T. J., Evans, J. G., Morison, J.
10 I. L., and Iamarino, M.: Effects of urban density on carbon dioxide exchanges: Observations of dense urban, suburban and
11 woodland areas of southern England, *Environmental Pollution*, 198, 186-200, 10.1016/j.envpol.2014.12.031, 2015.

12

13 Wennberg, P. O., Mui, W., Wunch, D., Kort, E. A., Blake, D. R., Atlas, E. L., Santoni, G. W., Wofsy, S. C., Diskin, G. S.,
14 Jeong, S., and Fischer, M. L.: On the sources of methane to the Los Angeles atmosphere, *Environmental Science &*
15 *Technology*, 46, 9282-9289, 10.1021/es301138y, 2012.

16

17 Wood, C. R., Lacser, A., Barlow, J. F., Padhra, A., Belcher, S. E., Nemitz, E., Helfter, C., Famulari, D., and Grimmond, C. S.
18 B.: Turbulent flow at 190 m height above London during 2006-2008: A climatology and the applicability of similarity theory,
19 *Boundary-Layer Meteorology*, 137, 77-96, 10.1007/s10546-010-9516-x, 2010.

20

21 Wunch, D., Wennberg, P. O., Toon, G. C., Keppel-Aleks, G., and Yavin, Y. G.: Emissions of greenhouse gases from a North
22 American megacity, *Geophysical Research Letters*, 36, 10.1029/2009gl039825, 2009.

23

24 Zazzeri, G., Lowry, D., Fisher, R. E., France, J. L., Lanoiselle, M., and Nisbet, E. G.: Plume mapping and isotopic
25 characterisation of anthropogenic methane sources, *Atmospheric Environment*, 110, 151-162,
26 10.1016/j.atmosenv.2015.03.029, 2015.

27

1 **Tables**

2 **Table 1: Annual totals of carbon dioxide flux and methane flux calculated from monthly averages for the period 2012-2014. The**
 3 **data period September 2012-March 2013 (no ultrasonic anemometer) was gapfilled using available monthly averages obtained over**
 4 **the remaining measurement period. Due to insufficient temporal coverage, individual annual budgets for 2012-2014 could not be**
 5 **derived for the carbon monoxide flux. A composite annual emissions estimate was compiled instead which makes use of all available**
 6 **monthly averages of F_{CO} over the study period September 2011 to December 2014. Data from the London Atmospheric Emissions**
 7 **Inventory (LAEI; emissions for the central London boroughs of Westminster and Camden) and previous measurement campaigns**
 8 **are provided for comparison with the current study.**

9

	Reference	F_{CO₂} [kt km⁻²]	F_{CH₄} [t km⁻²]	F_{CO} [t km⁻²]
2012	This study	40.2	69	-
2013	This study	40.7	75	-
2014	This study	36.3	72	-
Mean ± SD	This study	39.1 ± 2.4	72 ± 3	89
Random uncertainty	This study	6.5	12	16
Emissions inventory (2012)	LAEI	38.7	29	110
London 2007	(Helfter et al., 2011)	35.5	-	-
London	(Ward et al., 2015)	46.6		
London Autumn 2007/08	(Harrison et al., 2012)			150 - 220
London July 2012	(O'Shea et al., 2014) [‡]	29.0	66	106

10 [‡] Aircraft measurements.

11

12

13

1 **Table 2: Emission ratios from measurements and the London Atmospheric Emissions Inventory (LAEI). Measured quantities are**
 2 **mean, median and range of monthly emissions segregated by wind direction.**

Emission category	Zone	F_{CH4}/F_{CO2}	F_{CO}/F_{CO2}	F_{CO}/F_{CH4}
Measured (this study):				
	Mean	0.0019	0.0018	0.9739
	Median	0.0019	0.0021	1.1304
	Minimum	0.0017	0.0004	0.1972
	Maximum	0.0022	0.0027	1.5951
LAEI (all sources)	Central	0.0009	0.0039	4.1023
	Inner	0.0010	0.0024	2.4546
	Outer	0.0094	0.0018	0.1965
Domestic Coal	Central	-	-	-
	Inner	0.0020	0.0460	22.400
	Outer	0.0020	0.0460	22.414
Domestic Oil	Everywhere	0.0001	0.0006	4.0000
Domestic Gas	Everywhere	0.0001	0.0006	6.0375
Non-Domestic Gas	Everywhere	0.0001	0.0002	2.2642
Boilers	Central	0.0001	4E-05	0.3270
	Inner	0.0001	5E-05	0.3548
	Outer	0.0001	5E-05	0.3482
Gas Leakage	Everywhere	26.607	-	-
Non-Road Mobile Machinery, agriculture & other	Central	0.0002	0.0347	213.55
	Inner	0.0003	0.0377	119.75
	Outer	0.3525	0.0576	0.1633
Road - All Sources	Central	-	0.0021	-
	Inner	-	0.0013	-
	Outer	-	0.0013	-

3

4

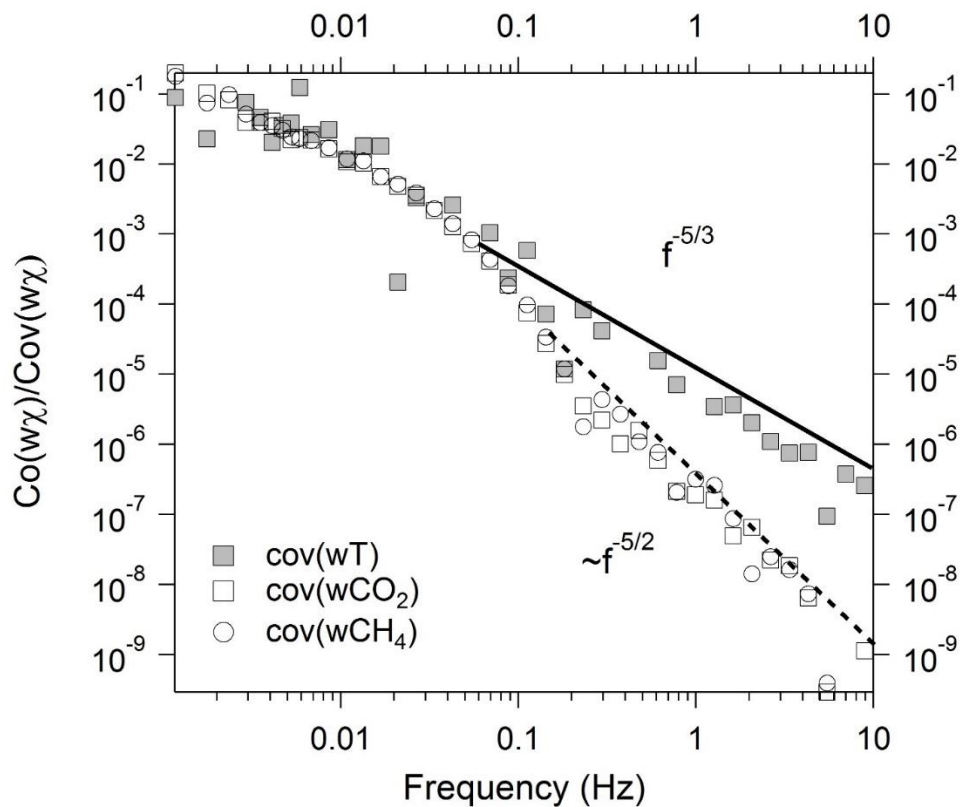
- 1 **Table 3: Goodness of fit of the linear regression between wind sector-segregated monthly methane fluxes (F_{CH_4}), carbon dioxide**
2 **fluxes (F_{CO_2}) and monthly mean air temperature (T_{air}). The superscripts (-) and (+) denote the sign of slope for each linear regression.**
3 **P-values in bold denote statistical significance.**

R^2	N	NE	E	SE	S	SW	W	NW
F_{CH_4} v. T_{air}	0.55 ⁽⁻⁾	0.43 ⁽⁻⁾	0.73 ⁽⁻⁾	0.08 ⁽⁻⁾	0.04 ⁽⁻⁾	0.05 ⁽⁻⁾	0.60 ⁽⁻⁾	0.21 ⁽⁻⁾
p-value	0.0060	0.0197	0.0004	0.3627	0.5150	0.4790	0.0033	0.1367
F_{CO_2} v. T_{air}	0.51⁽⁻⁾	0.69⁽⁻⁾	0.80⁽⁻⁾	0.19 ⁽⁻⁾	0.18 ⁽⁻⁾	0.27 ⁽⁻⁾	0.60⁽⁻⁾	0.34 ⁽⁻⁾
p-value	0.0203	0.0021	0.0003	0.1496	0.1984	0.1650	0.0081	0.0776

4
5
6
7
8

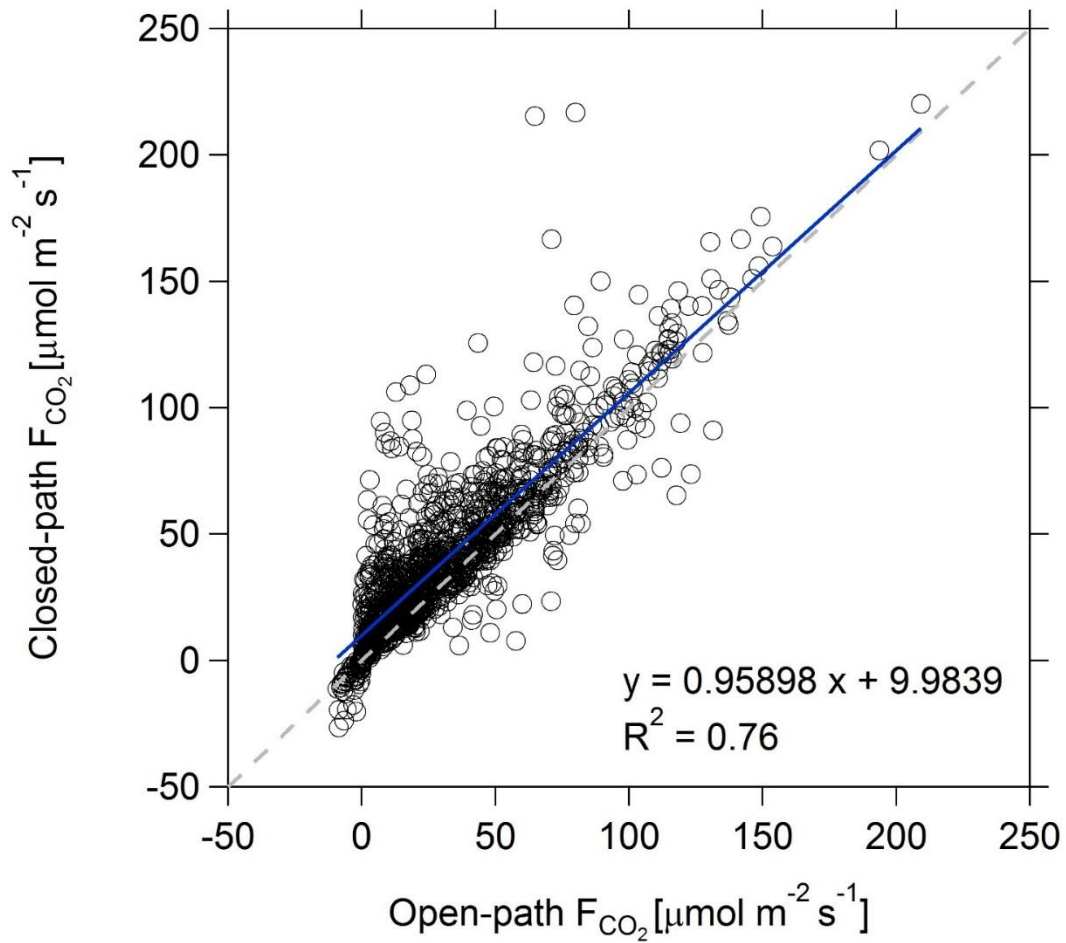
1 **Figures**

2



3

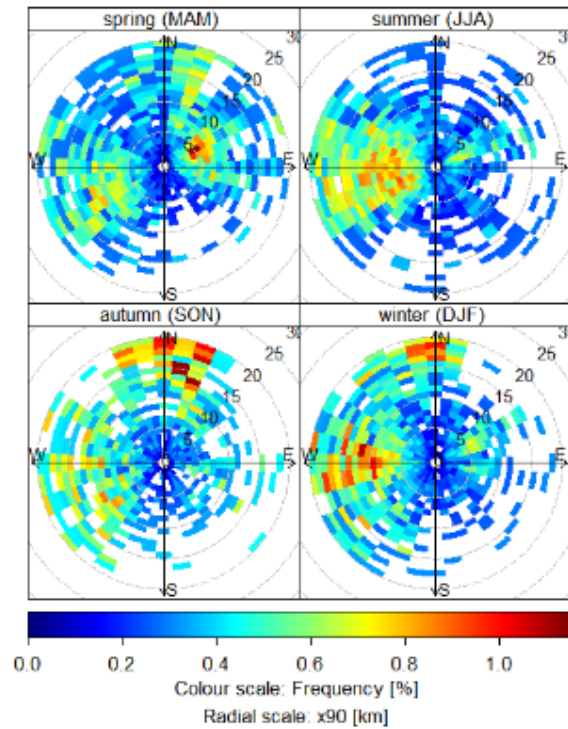
4 **Figure 1: Normalised cospectra of T (sonic temperature), CO₂ and CH₄ with respect to w (vertical wind component). Each**
5 **cospectrum is an average of 24 half-hourly cospectra (data period 12/03/2013 7:00 – 18:00). Regression of spectra for frequencies >**
6 **0.1 Hz marked by solid line for Co(wT) and dashed line for both Co(wCO₂) and Co(wCH₄).**



1

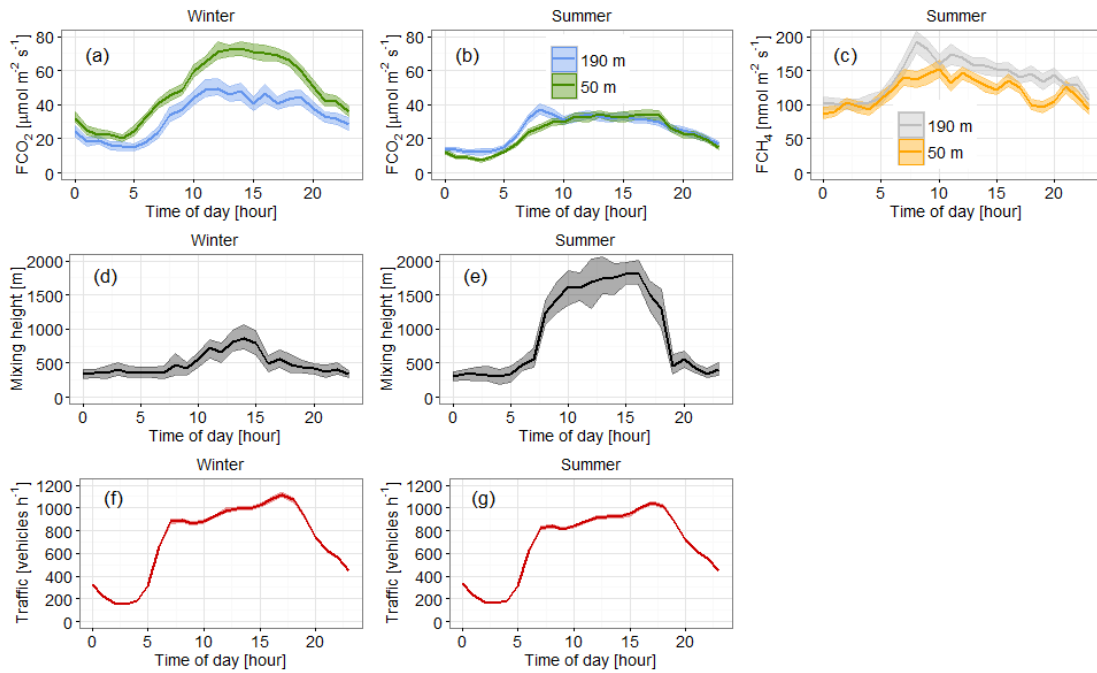
2 **Figure 2: Comparison of half-hourly fluxes of CO₂ measured in March, August and October 2013 by a closed-path Picarro G1301-**
 3 **f operating at 1 Hz following high-frequency loss correction and an open-path Li7500 analyser operating at 20 Hz at the top of BT**
 4 **tower (sensor height: 190 m a.g.l.). Dashed line is 1:1 line.**

5



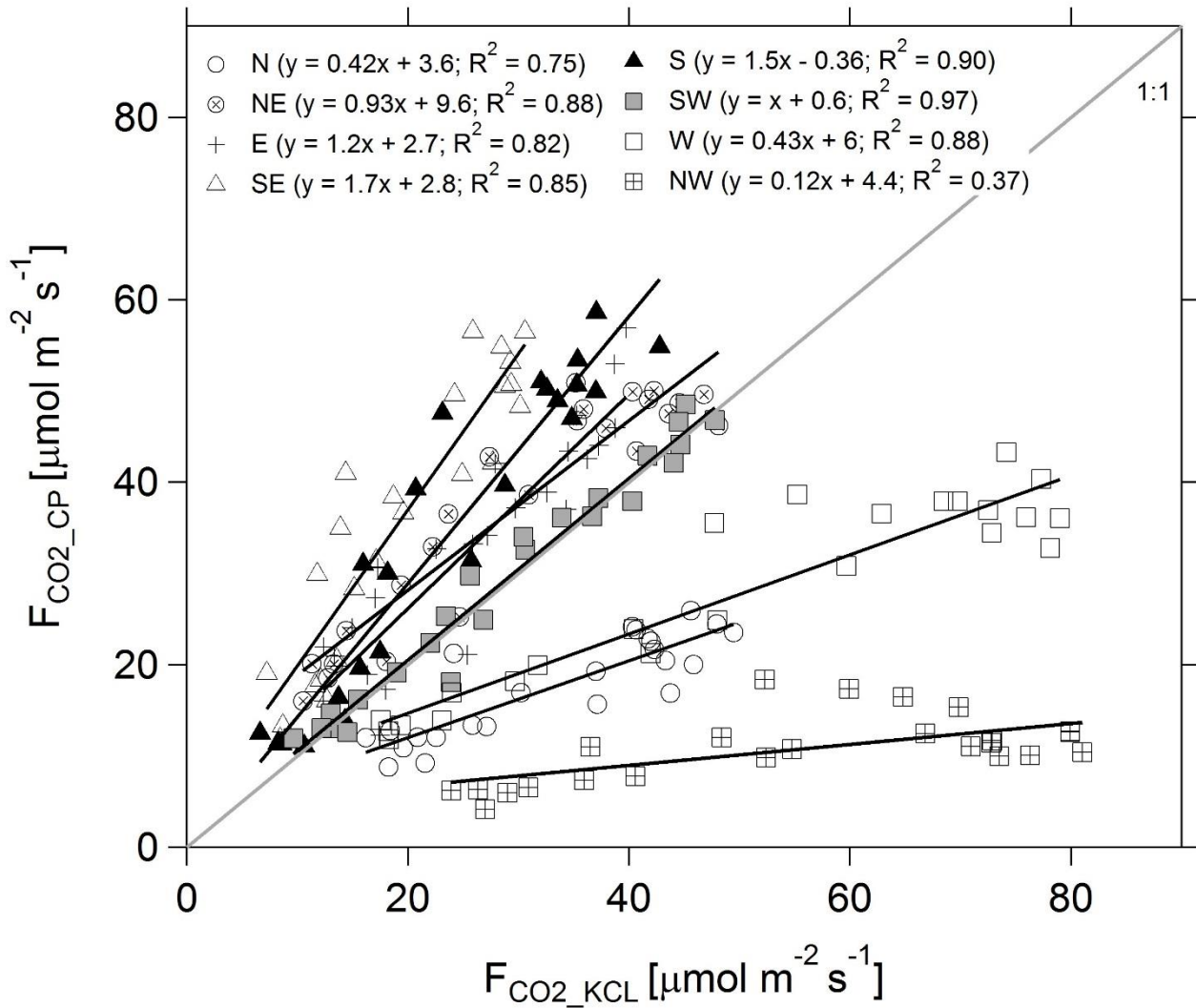
1
2
3
4
5
6
7
8
9
10

Figure 3: Frequency of occurrence of x_{90} (distance from the tower where 90% of the measured fluxes originated from) centred at the BT tower as a function of wind direction and season for the period 15/09/2011-31/12/2014. The flux footprint was estimated using an analytical model for non-neutral stratification (Kormann and Meixner, 2001) and the plots were produced using the openair package for R (Carlsaw and Ropkins, 2012; Carlsaw and Ropkins, 2016). Bin dimensions: 10° (angular scale) \times 1 km (radial scale).



1
2
3
4
5
6
7
8

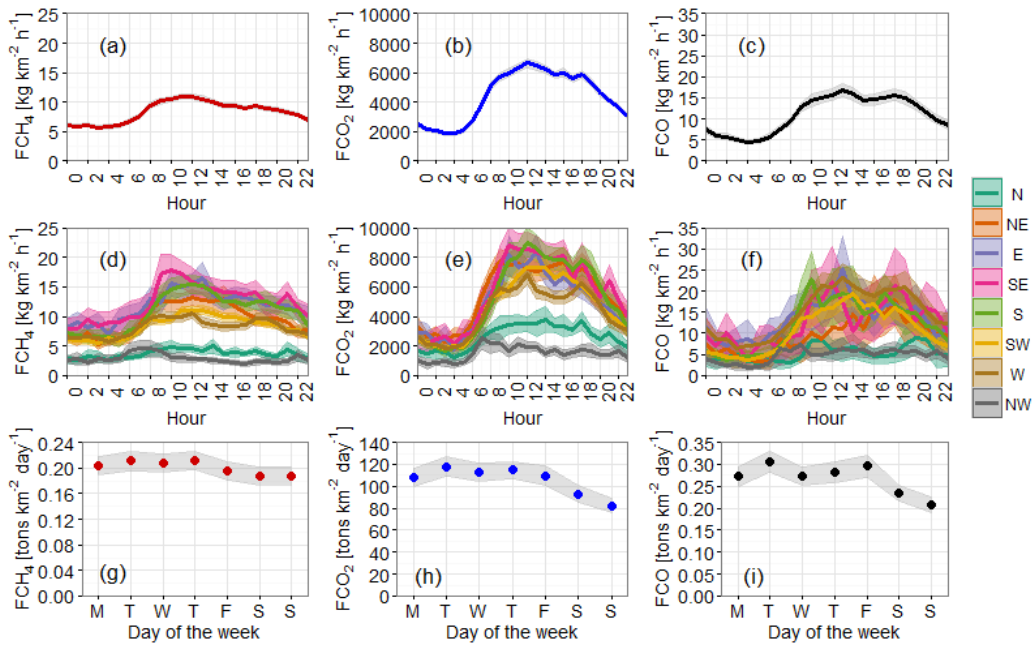
Figure 4: Mean diurnal profiles of CO₂ fluxes for (a) winter (DJF), and (b) summer (JJA) for the data period 15/09/2011 – 31/12/2013; (c) CH₄ fluxes in summer observed at the BT tower site (190 m a.g.l.) and the KCL site (50 m a.g.l.) over the period 19/08 – 01/10/2015; mixing height obtained from Doppler LIDAR measurements for (d) winter and (e) summer (Bohnenstengel et al., 2015); road traffic counts (f) winter and (g) summer (average of 246 counting stations distributed throughout the London conurbation; source: Transport for London, 2012 data). The shaded areas represent the 95% confidence interval.



1

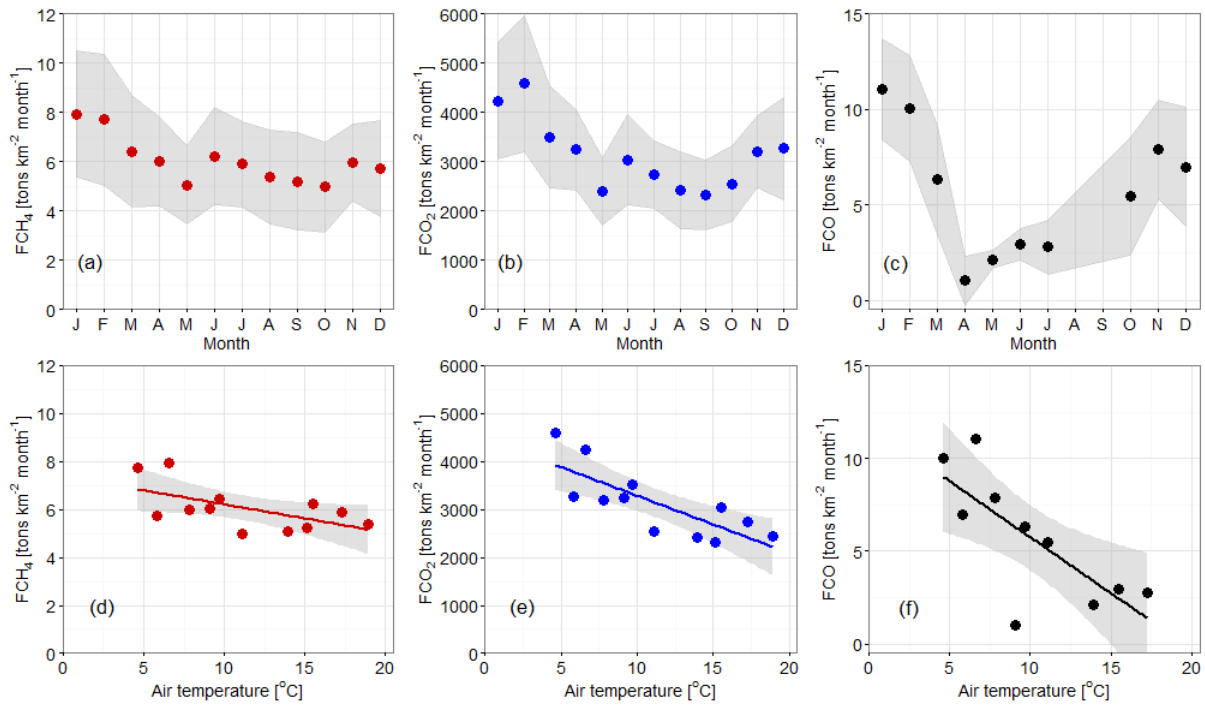
2 **Figure 5: Comparison between average diurnal profiles of CO₂ fluxes measured at the BT tower (190 m a.g.l.) and at the KCL site**
 3 **(50 m a.g.l.) in the period 15/09/2011 – 31/12/2013, separated into eight wind-direction sectors based on the wind direction observed**
 4 **at BT tower.**

5



1
2
3
4
5
6
7

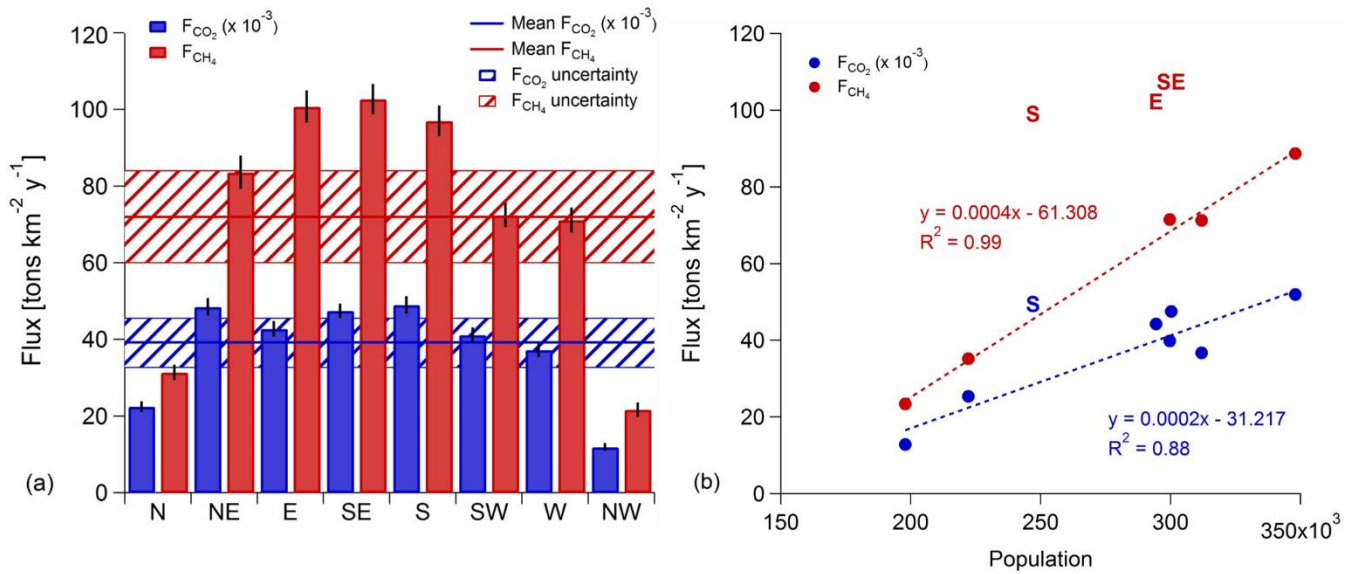
Figure 6: Fluxes of (a, d, g) methane (F_{CH_4}), (b, e, h) carbon dioxide (F_{CO_2}) and (c, f, i) carbon monoxide (F_{CO}) observed at BT tower with a closed-path gas analyser (from 15/09/2011 to 31/12/2014): (a)-(c) mean diurnal patterns with 95% confidence interval (shading), (d)-(f) as (a)-(c) but segregated into wind sectors and (g)-(i) by day of the week.



1
2
3
4
5

Figure 7: (a)-(c): Monthly averages of F_{CH_4} , F_{CO_2} and F_{CO} (September 2011-December 2014); (d)-(f): F_{CH_4} , F_{CO_2} and F_{CO} as a function of monthly mean air temperature. Solid lines are linear regressions and shaded areas are 95% confidence intervals. No F_{CO} measurements were available in August and September due to instrument downtime.

1



2

3 **Figure 8: Annual fluxes of carbon dioxide (F_{CO_2}) and methane (F_{CH_4}) measured by eddy-covariance at the BT tower in central**
 4 **London as a function of (a) wind direction; solid lines are mean annual emissions (2012-2014) without wind sector segregation.**
 5 **Measurement uncertainty (taken as the maximum of monthly uncertainties for each gas) is denoted by a blue (F_{CO_2}) and red striped**
 6 **areas (F_{CH_4}). (b) Data from plot (a) as a function of population within each wind sector-specific flux footprint area. The spatial extent**
 7 **of the footprint for each wind sector was derived from footprint statistics (Fig. 3) with the approximation that the typical extent was**
 8 **of the order of 10 km for NE-SW and 15 km for W-N. Population data (source: London Datastore, Greater London Authority, 2016)**
 9 **are on a ward basis (i.e. sub-borough administrative unit). Linear regression (dashed lines), with exclusion of S sector data point for**
 10 **F_{CO_2} , E, S and SE for F_{CH_4} (identified by their wind sector abbreviations). NB: F_{CO_2} and associated uncertainty are divided by 1000**
 11 **to aid visualisation.**

12